Catal Lett (2008) 126:200–206
DOI 10.1007/s10562-008-9607-1

Selective Oxidation of *n*-Pentane Over V_2O_5 Supported on Hydroxyapatite

Sooboo Singh · Sreekanth B. Jonnalagadda

Received: 4 June 2008 / Accepted: 31 July 2008 / Published online: 3 September 2008

Abstract The catalytic efficiency of V_2O_5 supported on hydroxyapatite in controlled oxidation of *n*-pentane to phthalic anhydride and maleic anhydride is investigated as function of flux rates of the reactants and temperature in the gas- phase in a fixed- bed stainless steel microreactor under steady state conditions. The hydroxyapatite was prepared by co-precipitation and the loaded catalysts by wet impregnation using NH_4VO_3 solution. Selectivity towards the products was influenced by the total flow rate, reaction temperature and V_2O_5 loadings. Good selectivities towards the anhydrides (MA 40% and PA 25%) is obtained with 5.0 and 7.5 wt.% of V_2O_5 at 360 °C.

Keywords V_2O_5 · Hydroxyapatite · Selective oxidation of *n*-pentane · Phthalic anhydride · Maleic anhydride

1 Introduction

Supported vanadium oxide catalysts have become an important class of catalysts because they exhibit excellent activity and selectivity for a variety of oxidation reactions including the selective oxidation of benzene, butane or pentane to maleic anhydride [1–3] and the conversion of *o*-xylene or naphthalene to phthalic anhydride [4, 5]. Phthalic anhydride (PA) and maleic anhydride (MA) are important chemical precursors used extensively for the synthesis of plasticizers required for the production of flexible PVC products, alkyd resins used in the manufacture of paints, dyes and pigments and also unsaturated polyester resins. It is generally accepted that *o*-xylene and *n*-butane are, respectively the preferred feed stocks for the production of PA and MA. However, the scope of *n*-pentane as feed stock has been recently explored. The oxidation of *n*-pentane over VPO, 12-molybdophosphoric acid, vanadomolybdophosphates, and vanadium-substituted molybdophosphoric acid resulted in more oxygenated products compared to only 10% of oxygenates found in the products for the oxidation of *n*-butane [6, 7]. This prompted Michalakos et al. [8] to study the variation in the selectivity for *n*-pentane on supported vanadia catalysts. In the preparation of these catalysts, vanadia was introduced by impregnating Al_2O_3 with a methanol solution of vanadium triisopropoxide and for SiO_2, an aqueous oxalic acid solution of ammonium metavanadate was used. The vanadia loadings for the Al_2O_3 samples were 8.2 and 23.4 wt.% V_2O_5 and for the SiO_2 samples were 1 and 10 wt.%. The Al_2O_3-supported catalysts were more active than the SiO_2-supported ones. For samples of the same support, the activity per mole depended slightly on the loading. At low pentane conversions, the 1 wt.% V/SiO_2 produced pentenes and 1,4-pentadiene, whereas the 10 wt.% V/SiO_2 produced, mainly carbon oxides and some MA. On the Al_2O_3- supported samples, there was no indication of dehydrogenated products. MA was produced with a selectivity of about 80% at low conversion on 23.4 wt.% V/Al_2O_3 but was a minor product on 8.2 wt.% V/Al_2O_3. Small amount of PA was observed on the Al_2O_3-supported samples and none was observed on the SiO_2- supported samples.

In this communication, we report the catalytic activity of different loadings of V_2O_5 supported on calcium hydroxyapatite for the selective oxidation of *n*-pentane. Calcium hydroxyapatites (HAp) are bifunctional materials with acidic or basic properties depending on their compositions, $[Ca_{10-x}(HPO_4)_x(PO4)_{6-x}(OH)_{2-x}, 0 \leq x \leq 1]$. Stoichiometric HAp has $x = 1$ to give $Ca_{10}(PO_4)_6(OH)_2$, whereas the

---

S. Singh · S. B. Jonnalagadda (✉)
School of Chemistry, University of KwaZulu-Natal,
Westville Campus, Chiltern Hills, Durban, South Africa
e-mail: jonnalagaddas@ukzn.ac.za

calcium deficient non-stoichiometric HAp has $0 \leq x \leq 1$ [8]. Hydroxyapatites are the main component of hard tissues, such as bone and teeth and, have found applications as materials in bioceramics, adsorbents, catalysts, and catalyst support materials [10].

2 Experimental

Calcium hydroxyapatite (HAp) was prepared according to methods of Yasukava et al. [11] and Gibson and Bonfield [12]. Concentrated NH_3 (BDH, Poole, England, AnalaR grade) was added to a 60 mL solution of $Ca(NO_3)_2 \cdot 4H_2O$ (6.67×10^{-2} mol) (Merck KGa, Darmstadt, Germany, GR for analysis) to elevate the pH to 11. The solution was then diluted to 120 mL with distilled water. Similarly, a 100-mL solution of $(NH_4)_2HPO_4$ (4.00×10^{-2} mol) (Merck KGa, Darmstadt, Germany, GR for analysis) was brought to pH 11–12. This solution was then diluted to 160 mL. The calcium solution was vigorously stirred at room temperature. The phosphate solution was added drop wise over a period of 30 min. A white, gelatinous precipitate formed which was stirred and boiled for 10 min. After filtration, the precipitate was washed thoroughly and dried in an oven set at 100 °C overnight and then calcined at 500 °C. Bulk V_2O_5 was prepared by the thermal decomposition of NH_4VO_3 (Merck KGa, Darmstadt, Germany) at 450 °C for 6 h in air. The loading of 2.5, 5.0, 7.5, 10.0 and 15.0 wt.% vanadia on the hydroxyapatite support was performed by wet impregnation. The desired amounts of V_2O_5 were suspended in 20 mL of distilled water and added to the calcium hydroxyapatite support. The water was removed by evaporation with constant stirring. The solid was dried overnight at 110 °C and later calcined at 500 °C for 6 h.

The BET surface area was carried out by degassing the catalysts under N_2 flow overnight at 250 °C using a Micrometrics Flow Prep 060. The degassed samples were analyzed in the Micrometrics Gemini 2360 (Micrometrics, USA), fully automatic, multi-point BET surface area analyzer under liquid N_2. Inductively coupled plasma (ICP) was performed using a Perkin Elmer Optical Emission Spectrometer Optima 5300 DV. Standards (500 ppm Ca, V and P) were purchased from Fluka, whereas the powder X-ray diffraction (XRD) was conducted on a Phillips PW 1830 X-ray diffractometer system, equipped with Co K_α radiation ($\lambda = 1.7889$). The infrared (IR) spectra were recorded on a Nicolet Impact 420 spectrophotometer in the mid IR (400–4,000 cm^{-1}) region using the KBr disc technique (0.5% dilution). TPR investigations were carried out with a custom made reactor system connected to a thermal conductivity unit. A 5% dihydrogen in argon mixture was used for the analysis.

The oxidation reactions were carried out in the gas phase in a continuous, fixed-bed tubular stainless steel microreactor (10 mm diameter and 300 mm length). Blank runs were carried out. After the blank runs, experimental runs were carried out using the materials V_2O_5 loaded on hydroxyapatite. The catalyst bed (2 mL) was located at the center of the reactor with carborundum packed in the spaces on either side of the bed. The reactor was heated in an electrical furnace. K-type thermocouples were used to monitor the temperature of the catalyst bed and the furnace. The thermocouples were controlled by CB-100 RK Temperature Control Units. The product stream was analyzed by Gas Chromatograph (Varian Star 3400) equipped with a FID module and GC–MS (Finnigan MAT GCQ) using capillary columns (J&W HP5- MS, 250 μm diameter). The carbon oxides and light organic compounds were continuously monitored by a TCD Gas Chromatograph (Buck Scientific, SRI Instruments, USA) using a packed column (6′silica gel/6′ molecular sieve). The selectivities were calculated from the conversion of *n*-pentane to every product on the basis of the number of carbons.

3 Results and Discussion

3.1 BET Surface Area and Elemental Analysis

Table 1 summarizes the surface areas and bulk compositions of the HAp and the six different V_2O_5 loadings (2.5–15%) on HAp support. The BET surface area of CaHAp of 48 $m^2\,g^{-1}$ agrees with that found in literature [13]. There is a decrease in the surface area of the materials from 37 to 9 $m^2\,g^{-1}$ with an increase in V_2O_5 content. This could be attributed to the clogging of the narrow pores of the support with the active component making it inaccessible to nitrogen molecules, leading to a decrease in the surface area. A slight difference in the surface areas was also noticed with the fresh and spent catalysts. The Ca/P ratio for HAp is 1.665 (Table 1) which indicates that stoichiometric hydroxyapatite was prepared. As the loading of vanadia on HAp increased the Ca/P ratio decreased resulting in calcium deficient HAp.

3.2 XRD Data

Figure 1a shows the XRD patterns of CaHAp. The XRD patterns of HAp confirm that the phases belong to stoichiometric hydroxyapatite with the formula, $Ca_{10}(PO_4)_6(OH)_2$ and they match well with the phases reported in literature [14]. V_2O_5 supported on HAp are displayed in Fig. 1b–f. The presence of crystalline V_2O_5 (▲) and VO_2 (■) phases were evident in all the catalysts.

Table 1 BET surface areas and bulk composition of the catalysts determined by ICP-OES for various V_2O_5/HAp catalysts

Catalyst	BET surface area		Ca/P	(V + Ca)/P	V/Ca
	Fresh ($m^2\ g^{-1}$)	Spent ($m^2\ g^{-1}$)			
HAp	48	46	1.665	–	–
2.5% V_2O_5/HAp	37	34	1.372	1.413	0.030
5.0% V_2O_5/HAp	26	22	1.405	1.544	0.099
7.5% V_2O_5/HAp	18	17	1.424	1.610	0.131
10.0% V_2O_5/HAp	11	7	1.463	1.754	0.199
15.0% V_2O_5/HAp	9	5	1.404	1.735	0.152

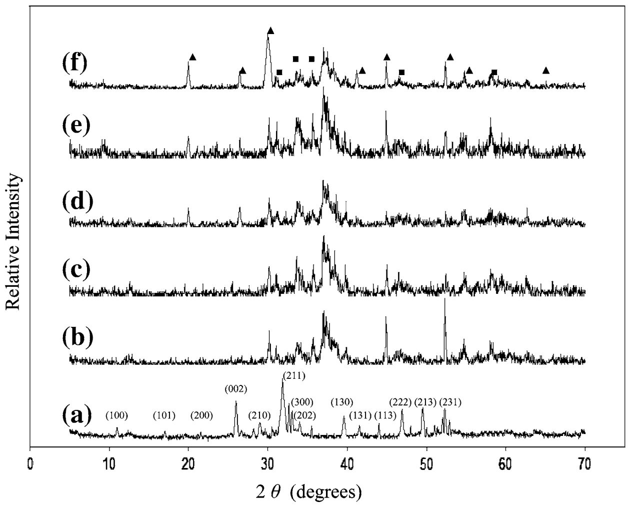

Fig. 1 XRD patterns of (**a**) HAp and (**b**) 2.5, (**c**) 5.0, (**d**) 7.5, (**e**) 10.0, (**f**) 15.0 wt.% V_2O_5 on HAp; crystalline V_2O_5 (▲), VO_2 (■)

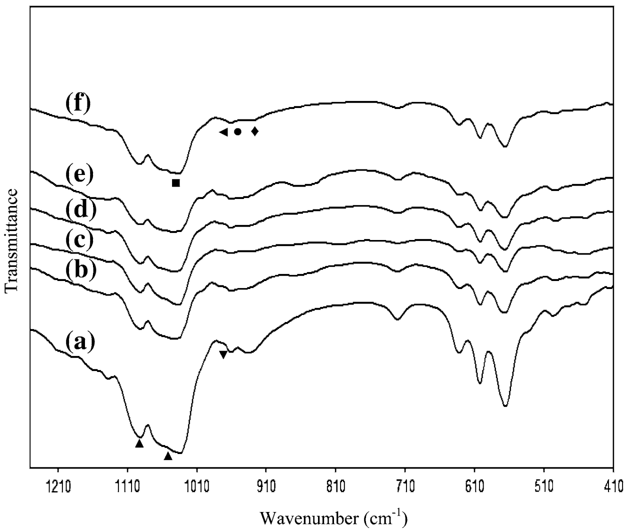

Fig. 2 Infrared spectra of (**a**) HAp and (**b**) 2.5, (**c**) 5.0 (**d**) 7.5, (**e**) 10.0, (**f**) 15.0 wt.% V_2O_5 on HAp

3.3 IR Spectra

The infrared spectrum of HAp confirms the formation of the hydroxyapatite structure (Fig. 2a). Typical bands were observed at 1,090 cm^{-1} (▲) and 1,040 cm^{-1} (▲) due to (ν_{as} (P–O)) and 960 cm^{-1} (▼) (ν_s (P–O)) [14]. For the V_2O_5 supported on the hydroxyapatites, the spectra are illustrated in Fig. 2b–f. Bands in the range 1,020–980 cm^{-1} are due to overtones and summation bands of the stretching modes of V=O in crystalline V_2O_5 (1,020 cm^{-1} (■) (strong), 980–985 cm^{-1} (◙) (shoulder)). An absorption at 940 cm^{-1} (◆) can be attributed to the symmetric stretch of V=O bonds in VO_x clusters and a band at about 980 cm^{-1} (●) due to the stretching frequency of VO_x surface species [15].

3.4 TPR Data

The temperature programmed reduction profiles for V_2O_5 and V_2O_5 supported on HAp are shown in Fig. 3. It can be seen that HAp is not reduced at the temperatures used [16]. The results also show single peak for the lower loadings due to the reduction of one type of species and the majority of the vanadia species are present as a monolayer strongly interacting with HAp, whereas samples containing 10.0 and 15.0 wt.% V_2O_5 present a peak and a shoulder. According to Bond et al. [17] and Dias et al. [18] the first peak can be attributed to VO_x monolayer species which are more reducible than pure V_2O_5. The shoulder detected for samples with higher V_2O_5 content is probably associated with small crystallites of V_2O_5. Also temperatures corresponding to the TPR peaks show an increase with V_2O_5 content. Bond et al. also suggested that this is probably due to the samples being prepared by the wet impregnation technique. It is also generally accepted that monomeric vanadates and polyvanadates chains are formed at low vanadia loading [19, 20]. When the concentration increases, polyvanadates chains condense to form surface vanadia monolayer and finally crystalline V_2O_5 appears for concentrations above the monolayer capacity. At lower loadings, reduction was around 500 °C, whereas good activity was obtained between 300 and 400 °C. The observed activity at the lower temperatures could be attributed to interaction of support with the vanadia and possible role of support in facilitating reduction at lower temperatures than 500 °C.

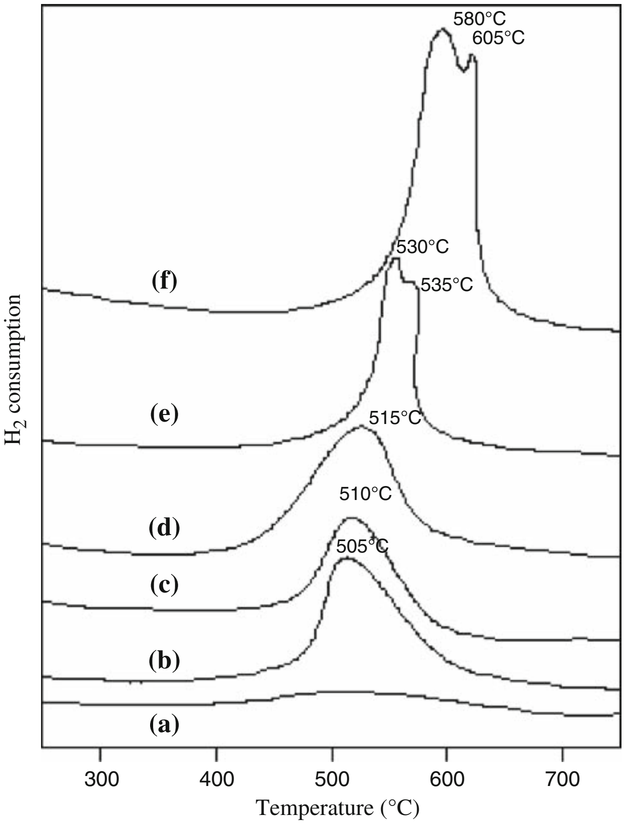

Fig. 3 Temperature programmed reduction profiles of V_2O_5/HAp catalysts; (**a**) HAp (**b**) 2.5 (**c**) 5.0 (**d**) 7.5 (**e**) 10.0, and (**f**) 15.0 wt.% V_2O_5/HAp

The selective oxidation of *n*-pentane using different weight percentages of V_2O_5 impregnated on HAp was investigated in a fixed-bed microreactor. The experiments were carried out at six different flow rates over a temperature range of 240–440 °C. Steady state was achieved after 3 h for each catalytic run. Blank runs carried out with the reactor filled with carborundum, showed negligible activity (1.0–2.5% conversion). The activity increased to 4.5–10.0% with the use of HAp as the catalyst. The products obtained consisted of lower hydrocarbons and oxygenated compounds, carbon oxides and very small amounts 1,3-pentadiene, furan, and furfural.

For the supported catalysts, experiments were conducted in duplicate with five loadings of vanadia (2.5, 5, 7.5, 10, and 15 wt.%) loaded on HAp support. With each loading, experiments were repeated at four Gas Hourly Space Velocities (GHSV = 1500, 1900, 2300, and 2700 h^{-1}) and each at six different temperatures, namely 240, 280, 320, 360, 400, and 440 °C. The product composition depended on the V_2O_5 loadings, the temperature and to a lesser extent on the GHSVs. All the analyzed data showing the conversions and selectivity towards different major products as function of vanadia loadings on the support, GHSVs and temperature conditions is summarized in five tables and provided for perusal as supplementary material.

Figure 4 shows representative results depicting the impact of temperature variation on the selectivity profiles of *n*-pentane oxidation products, when 2.5 wt.% V_2O_5 on HAp is used as catalyst at 2,700 h^{-1} GHSV. A perusal of the figure indicates that at lower temperatures selectivity towards benzoic acid and CO was high and decreased at higher temperature. The selectivity towards formation phthalic anhydride, maleic anhydride, and benzoic acid increased, reaching a maximum at different temperatures for each species.

The best results were obtained with V_2O_5 loadings of 5.0 and 7.5 wt.% at a temperature of 360 °C with GHSVs of 1900 and 2300 h^{-1}. The major compounds obtained were phthalic anhydride, maleic anhydride, carbon monoxide, carbon dioxide, and benzoic acid. The minor products positively identified and quantified were C_2–C_4 hydrocarbons, benzene, acetic acid, propanoic acid, 2-propenoic acid, 1,3-pentadiene, pentanoic acid, hexanal, 1,3- cyclobutanediol, 3,5-hexadien-2-ol, benzaldehyde, furan, 1,2- benzenedicarboxylic acid, and H_2O. Moisture content analyzed by Karl Fischer titration in most samples was negligible. A carbon mass balance of 100 ± 2.5% was obtained in all cases. Table 2 summarizes the analyzed data showing the conversions and product distribution for the partial oxidation of *n*-pentane at 320 and 360 °C. The conversion of *n*-pentane increased when the temperature was raised. At 360 °C with GHSV of 2300 h^{-1}, the 5.0 wt.% V_2O_5/HAp and 7.5 wt.% V_2O_5/HAp catalysts produced the maximum anhydride yields for a 63 and 78% conversion of feedstock, respectively. Significant amounts of carbon oxides were produced for all the V_2O_5 loadings.

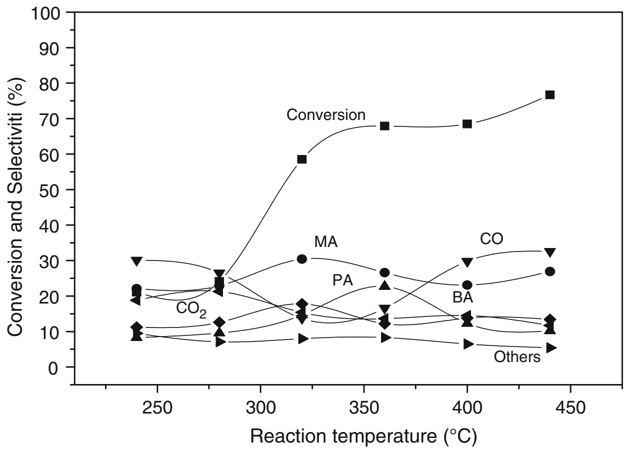

Fig. 4 Selectivity of various major products as a function of temperature (2.5 wt.% V_2O_5 on HAp at 2700 h^{-1} GHSV) MA = Maleic anhydride, PA = Phthalic anhydride, and BA = Benzoic acid

Table 2 Reaction data for the partial oxidation of *n*-pentane at 320 and 360 °C for GHSVs of 1900 and 2300 h^{-1}

Catalyst	Temperature (°C)	GHSV (h^{-1})	Concentration (%)	Selectivity(%)					
				MA	PA	CO	CO_2	BA	Others
2.5% V_2O_5/HAp	320	1900	55.2	32.7	6.4	32.1	15.2	8.2	5.4
		2300	52.3	19.6	19.5	24.6	18.5	9.6	8.2
	360	1900	73.7	30.1	12.9	34.6	12.6	5.5	4.3
		2300	64.1	36.2	16.3	17.3	10.3	11.8	8.1
5.0% V_2O_5/HAp	320	1900	60.8	21.6	8.6	34.7	23.4	3.6	8.1
		2300	53.6	29.2	16.5	26.9	11.6	10.2	5.6
	360	1900	71.2	30.2	11.7	32.1	20.1	2.4	3.5
		2300	63.0	40.4	24.2	16.5	10.5	5.6	2.8
7.5% V_2O_5/Hap	320	1900	61.5	25.9	13.9	33.2	19.6	3.9	3.7
		2300	62.2	22.3	14.8	25.8	17.4	14.6	5.1
	360	1900	79.3	34.2	18.2	24.5	7.2	7.3	8.6
		2300	77.8	41.1	25.2	16.3	12.1	1.9	3.4
10.0% V_2O_5/Hap	320	1900	67.0	30.9	24.1	15.6	16.3	4.2	8.9
		2300	62.0	19.9	15.8	24.5	16.6	15.1	8.1
	360	1900	74.7	35.7	23.2	17.7	14.2	3.3	5.9
		2300	70.4	30.9	17.6	23.9	10.3	9.7	7.6
15.0% V_2O_5/Hap	320	1900	66.8	22.7	20.3	29.7	14.6	5.2	7.5
		2300	65.4	18.6	13.7	35.9	15.9	9.6	6.3
	360	1900	77.9	26.2	19.6	30.4	13.6	5.4	4.8
		2300	76.9	25.2	19.4	28.6	9.6	7.6	9.6

MA = Maleic anhydride, PA = Phthalic anhydride, and BA = Benzoic acid

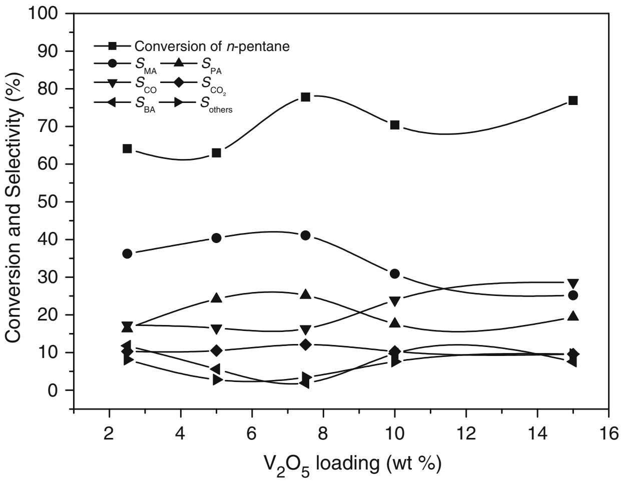

Fig. 5 Conversion and selectivity as a function of V_2O_5 loading for HAp supported V_2O_5 catalysts at 360 °C; GHSV = 2300 h^{-1}

Figure 5 illustrates the typical selectivity profiles of major products of the controlled oxidation of *n*-pentane as a function of V_2O_5 loading at 360 °C (GHSV = 2300 h^{-1}). Yields of up to 40% maleic anhydride were obtained with 5.0 and 7.5 wt.% V_2O_5 loadings and phthalic anhydride for corresponding conditions was 24 and 25%, respectively. The other V_2O_5 loadings also produced maleic anhydride and phthalic anhydride in generous amounts. When low yields of the anhydrides were obtained, a large amount of carbon oxides were produced. The opposite was true when large amounts of the anhydrides formed.

Using vanadia impregnated on alumina and silica supports for the selective oxidation of *n*-pentane Michalakos et al. [8] reported that the product selectivity depended on the vanadia loadings. In their studies, Al_2O_3-supported catalysts were more active than the SiO_2 supported ones. The selectivity of maleic anhydride was 14% selectivity for a 46% conversion of *n*-pentane at higher loading, and maleic anhydride was a minor product at lower loading. At low *n*-pentane conversions, the lower vanadia loadings on SiO_2 produced pentenes and 1,4-pentadiene, whereas the higher loading produced carbon oxides and some MA (23%). Small amounts of phthalic anhydride was observed in the product stream for the Al_2O_3- supported catalysts and none was observed for the SiO_2- supported samples. Owens and Kung [21] also reported the formation of dehydrogenation products for catalysts with lower loadings and about 13% maleic anhydride was detected for 8% conversion using a higher loaded sample.

In the current studies, much improved conversions (≈70%) with greater selectivity for anhydrides (maleic anhydride 40% and phthalic anhydride 25%) were

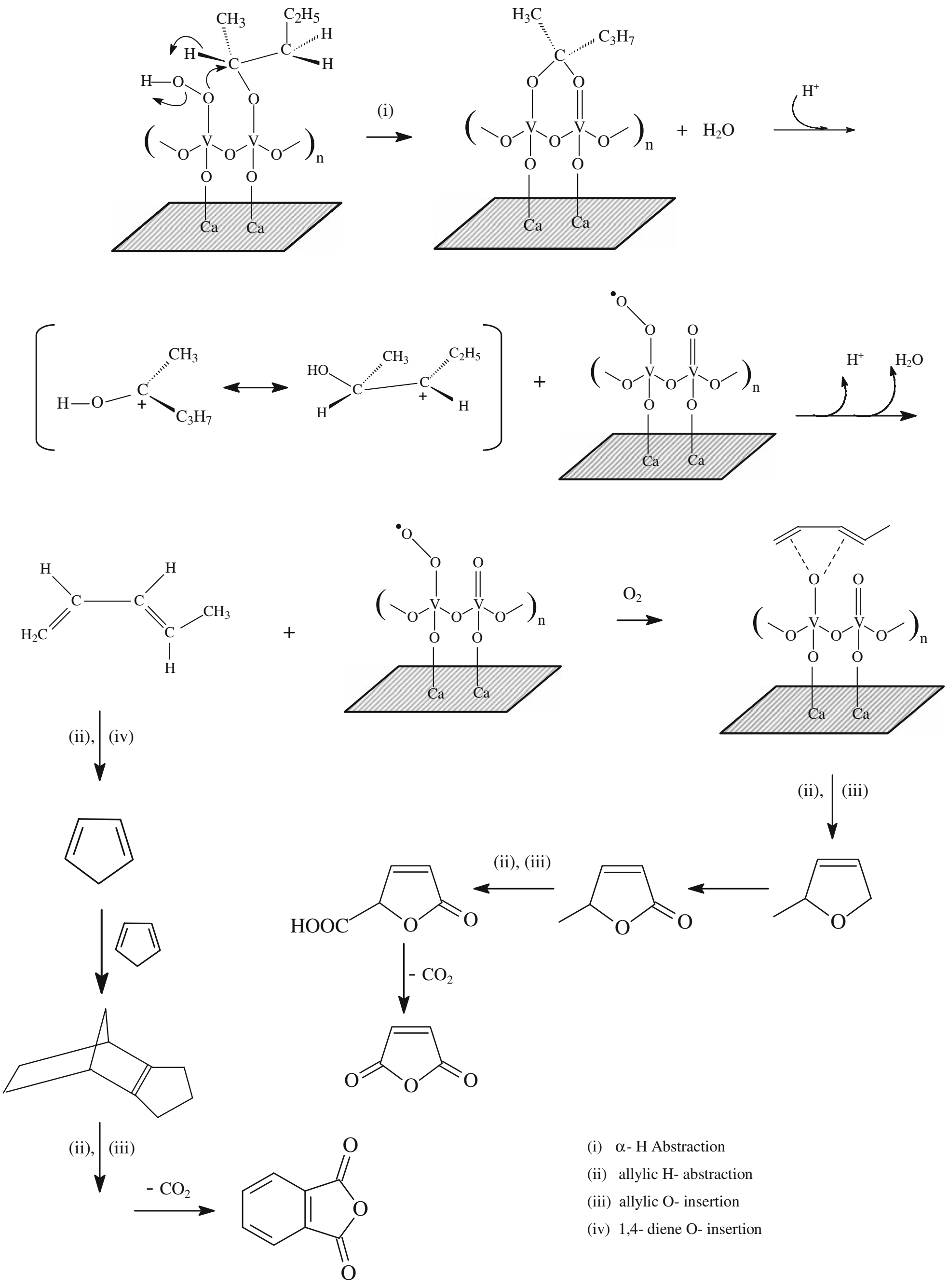

Scheme 1 Proposed mechanism for the formation of MA and PA from *n*-pentane over V_2O_5/HAp

achieved with V_2O_5 loaded on hydroxyapatite support compared to vanadia on alumina and silica supports for the selective oxidation of *n*-pentane [8].

The formation of a monolayer of vanadia and its interaction with support is of vital importance with respect to the activity of the catalyst. The vanadia moiety attaches as polymeric tetrahedral VO_4 units on the support [22]. As the initial step of catalysis the α-carbon of *n*-pentane attaches itself to the vanadyl oxygen on the active site.

Scheme 1 illustrates a proposed mechanism for selective oxidation of *n*-pentane to maleic anhydride and phthalic anhydride. The hydrocarbon is first oxydehydrogenated forming pentene and oxidized to pentadiene. Pentadiene is found among reaction intermediates. Pentadiene is then cyclized either via an allylic H—abstraction or the unsaturated C_5 compound is oxidized to maleic anhydride. The pentadiene also gets converted to cyclopentadiene, which dimerizes to a cyclic template and is finally oxidized to phthalic anhydride. During studies on the oxidation of *n*-pentane to anhydrides using vanadium phosphorus oxide as catalyst, Centi and Trifirò [23] also proposed a similar mechanism involving the dehydrogenation of *n*-pentane followed by formation of an olefin as intermediate in route to the anhydride formation.

4 Conclusions

From elemental analysis, the Ca/P ratio for HAp was 1.665 which confirms that stoichiometric hydroxyapatite was synthesized. Blank reactions using only HAp resulted in conversions of the feed up to about 10%, which indicate that the support itself has some activity. Hence, the catalytic efficiency is the resultant of enhanced activity due the vanadia and support interactions. Catalysts with 5.0 and 7.5 wt.% V_2O_5 loadings resulted in maleic anhydride yields of 40% and the formation of 25% for an average *n*-pentane conversion of 65%. Compared to the commonly used silica- and titania-supported catalysts [8, 21], there is a significant increase in the conversion of *n*-pentane to maleic anhydride and phthalic anhydride using the HAp-supported catalysts.

Acknowledgments Authors thank the University of KwaZulu-Natal and the National Research Foundation (Thuthuka), Pretoria for financial assistance.

References

1. Nikolov V, Klissurski D, Anastasov A (1991) Catal Rev Sci Eng 33:319
2. Guliants VV, Benziger JB, Sundaresan S, Wachs IE, Jehng J-M, Roberts JE (1996) Catal Today 28:275
3. Sananés MT, Hutchings GJ, Volta J-C (1995) J Catal 154:253
4. Dias CR, Portela MF, Bond GC (1995) J Catal 157:344
5. Dias CR, Portela MF, Banãres MA, Galán-Fereres M, López-Granados M, Peña MA, Fierro JLG (2002) Appl Catal A: Gen 224:141
6. Centi G, Lopez-Nieto J, Pinelli D, Trifirò F (1989) Ind Eng Chem 349 Res 28:400
7. Centi G, Trifirò F (1988) Catal Today 3:151
8. Michalakos PM, Birkeland K, Kung HH (1996) J Catal 158:349
9. Sugiyama S, Miyamoto T, Hayashi H, Moffat JB (1998) J Mol Catal A: Chem 135:199
10. Jun JH, Lim TH, Nam S-W, Hong S-A, Yoon KJ (2006) Appl Catal A: Gen 312:27
11. Yasukawa A, Kidokoro M, Kandori K, Ishikawa T (1997) J Colloid Inter Sci 191:407
12. Gibson IR, Bonfield W (2002) J Mater Sci: Mater Med 13:685
13. Venugopal A, Scurrel MS (2003) Appl Catal A: Gen 245:137
14. Parhi P, Ramanan A, Ray AR (2006) Mater Lett 60:218
15. Chary KVR, Kishan G, Bhaskar T, Sivaraj C (1998) J Phys Chem B 102:6792
16. Sebti S, Tahir R, Nazih R, Saber A, Boulaajaj S (2002) Appl Catal A: Gen 228:155
17. Bond GC, Perez Zurita J, Flamerz S, Gellings PJ, Bosch H, Van Ommen JG, Kip BJ (1986) Appl Catal 22:361
18. Dias CR, Portela MF, Bond GC (1995) J Catal 157:353
19. Bosch H, Kip BJ, van Ommen JG, Gellings PJ (1984) J Chem Soc Faraday Trans 180:2479
20. Wachs IE, Weckhuysen BM (1997) Appl Catal A: Gen 157:67
21. Owens L, Kung HH (1993) J Catal 144:202–213
22. Guliants VV (1999) Catal Today 51:255–268
23. Centi G, Trifirò F (1990) Chem Eng Sci 1990 45:2589–2596